

1 **Ultrasound Mediated Delivery of Quantum Dots from a** 2 **Capsule Endoscope to the Gastrointestinal Wall**

3 Fraser Stewart^{1,2,*+}, Gerard Cummins^{*3+}, Mihnea V. Turcanu⁴, Benjamin F. Cox⁵, Alan Prescott¹, Eddie
4 Clutton⁶, Ian P. Newton¹, Marc P.Y. Desmulliez⁷, M. Thanou⁸ H. Mulvana⁹, Sandy Cochran⁴ and Inke
5 Nätke¹

6 1 The University of Dundee, School of Life Sciences, Dundee, DD1 5EH, United Kingdom

7 2 The University of Strathclyde, Department of Electronic and Electrical Engineering,
8 Glasgow, G1 1XQ, United Kingdom

9 3 The University of Birmingham, School of Engineering, Birmingham, B15 2TT, United
10 Kingdom

11 4 The University of Glasgow, School of Engineering, Glasgow, G12 8QQ, United Kingdom

12 5 The University of Dundee, School of Medicine, Dundee, DD1 5EH, United Kingdom

13 6 The University of Edinburgh, The Roslin Institute, Edinburgh, EH25 9RG, United Kingdom

14 7 Heriot-Watt University, School of Engineering and Physical Sciences, Edinburgh, EH14
15 4AS, United Kingdom

16 8 Kings College London, Institute of Pharmaceutical Science, London, SE1 1DB, United
17 Kingdom

18 9 The University of Strathclyde, Department of Biomedical Engineering, Glasgow, G1 1XQ,
19 United Kingdom

20

21 *G.Cummins@bham.ac.uk

22 ^ fraser.stewart.101@strath.ac.uk

23 +these authors contributed equally to this work

24

1 **Abstract**

2 Biologic drugs, defined as therapeutic agents produced from or containing components of a living
3 organism, are of growing importance to the pharmaceutical industry. Though oral delivery of
4 medicine is convenient, biologics require invasive injections because of their poor bioavailability
5 via oral routes. Delivery of biologics to the small intestine using electronic delivery with devices
6 that are similar to capsule endoscopes is a promising means of overcoming this limitation and does
7 not require reformulation of the therapeutic agent. The efficacy of such capsule devices for drug
8 delivery could be further improved by increasing the permeability of the intestinal tract lining with
9 an integrated ultrasound transducer to increase uptake. This paper describes a novel proof of concept
10 capsule device capable of electronic application of focused ultrasound and delivery of therapeutic
11 agents. Fluorescent markers, which were chosen as a model drug, were used to demonstrate in-vivo
12 delivery in the porcine small intestine with this capsule. We show that the fluorescent markers can
13 penetrate the mucus layer of the small intestine at low acoustic powers when combining
14 microbubbles with focussed ultrasound. These findings suggest that the use of focused ultrasound
15 together with microbubbles could play a role in the oral delivery of biologic therapeutics.

16

17 **Introduction**

18 Oral delivery of therapeutic agents is generally the preferred route of administration due to increased
19 patient acceptance¹ and convenience compared to parenteral routes. Many pharmaceuticals, once
20 swallowed, are absorbed in the gastrointestinal (GI) tract, usually in the small intestine, which has
21 greater absorptive capacity than other parts of the GI tract due to factors such as its length and
22 surface area of up to 6 m and 200 m² respectively in adults². However, the challenging environment
23 of the GI tract limits the successful absorption, and the ability to establish sufficient systemic levels
24 of therapeutics. The pH along the gastrointestinal (GI) tract varies widely, and the gut contains many

1 enzymes that reduce the stability, bioavailability, and thus effective delivery of many
2 biomacromolecules^{3,4}. There are also physical barriers to uptake that must be overcome before any
3 biomacromolecular drugs can pass through the walls of the GI tract and reach the desired site in the
4 body. First, the drugs must pass through the mucus that coats the intestinal epithelium⁵. Then, they
5 must breach the barrier provided by the epithelial layer, specifically tight junctions between adjacent
6 epithelial cells. These and other constraints have limited oral drug delivery to small molecules⁴. A
7 more effective GI drug delivery system should achieve efficient delivery of a broader class of
8 therapeutic agents, including biologics, with increased bioavailability and minimized toxic side
9 effects and a reduction in the quantity that needs to be administered. Such a system should also
10 remove the need for significant reformulations of the drugs and, for gastrointestinal diseases, enable
11 localized treatment of conditions such as inflammatory bowel disease (IBD)⁶.

12
13 Pharmaceutical technologies such as multilayered tablets, intestinal patches, microneedle patches,
14 hydrogels, and exosomes provide a means of controlling drug delivery in the intestine⁷. However,
15 these methods may require the reformulation of therapeutic agents to guarantee compatibility with
16 the chosen technique and ensure the efficacy of the drug⁸ though these methods are still not useful
17 to ensure effective oral delivery of biologicals.

18
19 Another strategy for more effective oral drug delivery has emerged from advances in electronic
20 miniaturization, specifically the development of capsule endoscopy (CE). Endoscopic capsules can
21 be swallowed, and they contain a camera and associated electronic subsystems that allow optical
22 imaging of the GI mucosa⁹. Clinical use of such capsules, primarily for the detection of occult GI
23 bleeding, has increased since their introduction in the early 1990s⁹. The ability of CE to transit the

1 entire GI tract makes them particularly suitable for imaging diseases that affect remote sections of
2 the small bowel.

3

4 Capsule endoscopy, mainly used for its diagnostic advantages, is also widely recognized as a
5 platform with therapeutic potential for the electronic delivery of commonly ingested drugs³. Capsule
6 endoscopes could transport and release any drug to a region of the GI tract within a specified time
7 after ingestion or upon detection of a change in pH. The clinical potential¹⁰ of such systems is
8 illustrated by positive results obtained from clinical trials with existing drug delivery capsules such
9 as Intellicap¹¹, Intellisite¹², and Enterion¹³. However, the potential of capsule devices for therapeutic
10 applications goes further, as they could also be modified to improve the bioavailability of drugs by
11 actively increasing tissue layer permeability. This approach would enhance the passage of
12 therapeutic agents across tissue barriers to allow more efficacious treatments and reduction in doses
13 that need to be delivered⁴.

14

15 Increased and reversible permeabilization of the tissue layers lining the GI tract can be induced
16 through the use of ultrasound (US)¹⁴⁻¹⁶. Ultrasound-mediated targeted delivery was first considered
17 in the 1980s as a method for targeting and enhancing therapeutic agent delivery¹⁷, with Phase III
18 clinical trials currently underway for one of the first clinical treatments using this technique¹⁸.
19 Conventional ultrasound-mediated targeted drug delivery (UmTDD) systems typically consist of an
20 extracorporeally situated US transducer coupled to the skin with water or gel and aimed toward a
21 target site¹⁹. Though this approach is not constrained by transducer size or power budget, the
22 presence of bone or gas in the path of the US beam can produce unintended hotspots and shadows,
23 and the patient must remain still to maintain the focus of the beam on the desired target.

24

1
2 US contrast agents, such as microbubbles (MBs), can be used to amplify these biophysical effects,
3 enabling ultrasound-induced reversible permeabilization of cell membranes at low acoustic powers.
4 Microbubbles consist of an inert gas core stabilized by a lipid or polymer shell typically 0.8-10 μm
5 in diameter²⁰. Several papers have demonstrated the ability of MBs to amplify the biophysical
6 effects of ultrasound, such as cavitation. The gas-filled, compressible core of MBs makes them
7 responsive to ultrasound, causing them to compress and expand alternately. This cyclical behavior
8 can increase cell permeability due to the formation of pores caused by either the interaction between
9 microbubbles and cell membranes at low acoustic pressures, referred to as stable cavitation, or
10 through shockwaves generated by the collapse of microbubbles proximal to the cell membrane
11 under high acoustic pressures, referred to as inertial cavitation¹⁴.

12
13 Some of the challenges associated with conventional UmTDD could be solved by placing the US
14 transducer intracorporeally. This approach achieved a tenfold increase in the permeation of the anti-
15 inflammatory drug 5-aminosalicylic acid when administered rectally²¹. However, in this case, the
16 size of the device limited positioning to the rectum only.

17
18 Therapeutic intervention using UmTDD along the entire length of the GI tract could be achieved by
19 placing the US source in a device resembling a CE. Such a device would also remove limitations
20 caused by patient movement, obstruction by bone or gas associated with extracorporeal US.
21 Intracorporeal UmTDD requires the miniaturization of the US transducer, resulting in lower power
22 consumption, a reduction of the US intensity, and a decrease in the therapeutic efficiency of the
23 treatment. However, the extent of these effects can be mitigated using MBs. The ability to increase

1 cell permeability at low acoustic pressures due to the interaction between MBs and the cells is
2 essential for the successful operation of an UmTDD capsule.

3

4 Following previous work²²⁻²⁴, this paper describes the design, manufacture, and characterization of
5 a proof-of-concept therapeutic capsule for ultrasound-mediated delivery of agents using MBs.
6 Previous work demonstrated that MBs, in conjunction with focused US reduced barrier function
7 more effectively than insonation or MBs alone in Caco-2 cell monolayers²⁴. Importantly, the
8 decrease in TEER was temporary, and TEER to normal values was rapidly restored after insonation
9 stopped. New results present the design of a new and more effective ultrasound-mediated delivery
10 capsule that can successfully deliver fluorescent particles using MBs and insonation to *ex vivo* and
11 *in vivo* tissues. The results of the *in vivo* experiments demonstrate that fluorescent markers can
12 penetrate the mucus layer lining the small intestine, illustrating the potential for a new method of
13 GI drug delivery.

14

15 **Results**

16 **Ultrasound Transducer Physical Characteristics**

17 A spherically focused US transducer with an outer diameter of 5 mm, a radius of curvature of 15
18 mm, and a central hole 1 mm in diameter was created using PZ26 piezoceramic material (Figure 1a).
19 The US was focused to create bioeffects in the focal region of the transducer. The central hole
20 facilitated the integration of the MB/drug delivery channel and simplified this new capsule design²³

21

1 **Ultrasound Transducer Fabrication and Characterisation**

2 Electrical impedance spectroscopy with a 4395A Impedance Analyzer (Keysight Technologies,
3 Santa Clara, CA, USA) established that the central operating frequency of the transducers, when
4 submerged in water, was 3.98 MHz. The magnitude of the electrical impedance at this frequency
5 was within 10% of the electrical impedance of the attached power cable; therefore, no electrical
6 matching was required. Acoustic output power measurements were performed with an input power
7 (W_{IN}) in the range of 20.1 mW to 223.6 mW. Results are shown in Table 1 and Table 2 for the
8 transducers used for the *ex vivo* tissue and *in vivo* porcine experiments respectively, with a minimal
9 difference in output power (W_{OUT}) for the two transducers. The beam diameter of the transducer at
10 -6 dB was measured using a commercial US field mapping (USFM) measurement system (Precision
11 Acoustics Ltd., Dorchester, England).

12
13 Acoustic pressure generated by the focused US transducer ranged from 308 ± 58.5 kPa to $1100 \pm$
14 209.1 kPa, and the beam diameter at - 6 dB was 1.38 mm. Output power (W_{OUT}) generated by the
15 transducer ranged from 12.8 ± 1.0 mW to 115 ± 8.1 mW. The efficiency of the transducer ranged
16 from 50.0 ± 5.0 to $64.0 \pm 5.2\%$, with an average of 54.2%. Focal plane intensities (IAC) were
17 measured to range between 1.0 ± 0.1 Wcm⁻² and 7.8 ± 0.5 Wcm⁻².

19 **Benchtop testing of Ultrasound-mediated Delivery Transducers in *Ex Vivo* Tissue**

20 Previous work demonstrated that uptake of fluorescent particles by monolayers of Caco-2 cells
21 could be enhanced by insonation²⁴. Measuring the efficacy of this method in tissue is a crucial step
22 towards its deployment *in vivo*. As in the earlier work with cells, quantum dots (QDs) were chosen
23 as the particles used to measure uptake/delivery. Quantum dots are fluorescent semiconductor

1 nanocrystals and are frequently used in imaging. They have broad excitation spectra, narrow
2 emission spectra, exhibit almost no photobleaching, and have long fluorescence lifetimes²⁵.

3

4 The small intestine was isolated from wild type (WT), and $Apc^{Min/+}$ mice and QDs were delivered
5 to the tissue. $Apc^{Min/+}$ mice are heterozygous for mutations in the adenomatous polyposis coli gene
6 (*Apc*) and are a well-established model of human familial adenomatous polyposis (FAP). FAP
7 patients are also heterozygous for mutations in *Apc* and develop numerous polyps in their intestinal
8 tract that progress to cancers if left untreated²⁶. $Apc^{Min/+}$ mice thus present a precancerous state.
9 They also have reduced mucus production²⁷, and any differences between WT and $Apc^{Min/+}$ tissues
10 could reflect differences in the mucus layer and/or changes associated with the epithelium in
11 precancerous tissue²⁸. The presence of QDs was compared in the samples with and without
12 insonation and between healthy and precancerous tissues.

13

14 Successful delivery of QDs was recorded when the fluorescence emitted by the QDs was detected
15 in the insonated area. In 11 of the 14 WT samples, fluorescence consistent with the accumulation
16 of QDs within insonated areas was observed (Figure 2a), corresponding to a success rate of 79%.
17 Accumulation of QDs was detectable in only 50% of the 14 $Apc^{Min/+}$ samples. This observation,
18 together with the fact that QD fluorescence was not observed after tissue samples were left in buffer
19 (PBS) for more than 2 hours and the reduced mucus layer reported in $Apc^{Min/+}$ tissue, suggested that
20 QDs were lodged in the mucus and did not reach the epithelial cells.

21

22 Experiments were also conducted on sections of WT porcine small intestine *post mortem*. These
23 tissue samples were obtained and used within 20 minutes of death to minimize tissue degradation.
24 Inspection of the porcine bowel samples exposed to QDs showed that QDs were detected only in

1 insonated areas of bowel tissue and not in control areas (Figure 2b). Of the 16 WT porcine samples,
2 12 were observed to emit fluorescence within insonated areas but not control areas reflecting a
3 success rate of 75% for *ex vivo* porcine samples.

4
5 Further murine experiments were conducted to measure the depth of penetration of the QDs in the
6 insonated region when ultrasound was used in conjunction with MBs. Laser scanning confocal
7 microscopy of the cross-sections of fixed murine intestinal tissue was used to determine the depth
8 of penetration of QDs after insonation with MBs. QDs (Figure 3, green) were enveloped in the
9 mucus layer (Figure 3, red), and but were not present in the cells in the underlying intestinal
10 epithelial tissue (Figure 3, nuclei stained blue), demonstrating that insonation was sufficient only to
11 drive the QDs into the mucus layer. This was further confirmed by examining a total length of
12 sections covering 41,400 μm of insonated tissue and failing to find QDs inside cells. Processing of
13 the tissue for staining caused the loss of much of the mucin, and only a few QDs remained with an
14 occasional QD inside folds of villi where mucus may also have been trapped.

15

16 ***In vivo* Testing of Ultrasound-mediated Delivery Capsule**

17 To determine the ability of our system to deliver reagents in live animals, five tissue samples were
18 collected from three pigs. Two additional samples from a fourth pig were excluded because these
19 cases, debris consumed naturally by the animal before the experimental period was found lodged in
20 the transducer channel when the capsule was removed from the small intestine. Such debris can
21 impede US and QD delivery and produce artificial results. As shown previously²⁹, fluorescence
22 associated with QD was detected in samples subjected to the MB/QD solution and US in the
23 insonated regions (Figure 4a) in four of the five samples, while no fluorescence was associated with
24 those samples subjected to just insonation (Figure 4b) or QDs (Figure 4c). Regions insonated in

1 conjunction with MB/QD delivery were positive for fluorescence, and non-insonated controls were
2 negative, corresponding to a success rate of 80%. High-resolution immunofluorescence imaging
3 suggested that the QDs were lodged in the mucus layer based on the similarity between images
4 obtained from murine and porcine benchtop trials (*ex vivo* tissue) (Figure 4d, 4e).

6 **Discussion**

7 Our results provide the first demonstration of *in vivo* of ultrasound-mediated delivery of an agent in
8 the small bowel using a proof-of-concept tethered endoscopic capsule. We attribute the higher
9 success rate for delivery to WT murine tissue (79%) compared to *Apc^{Min/+}* tissue (50%) to the lower
10 mucus production in the latter. Together our observations suggest that a capsule can successfully
11 drive fluorescent QDs into the mucus of the mucosal layer of the small intestine when applying
12 ultrasonic insonation together with MBs. The duration that the fluorescent particles persist in the
13 mucosa will be affected by the rate of continual mucus secretion and mucosal cell shedding.

14
15 Further work is needed to determine for how long the particles remain embedded in the mucus
16 before diffusing away and whether this residence time varies with the location along the GI tract³⁰.
17 MBs can attenuate and scatter ultrasound, making them effective as ultrasound imaging contrast
18 agents³¹. Though it will be challenging, further work is also needed to fully characterise the
19 relationship between drug uptake in tissue, incident ultrasonic energy and the local concentration of
20 MBs due to their ability to attenuate and scatter the incident ultrasound. This work complements
21 previous attempts to deliver material to the mucosa with UmTDD, which were limited to the rectum
22 due to the size of the system employed²¹. Furthermore, this work demonstrates the potential of
23 capsule-based, UmTDD devices for accessing the small bowel and transfer exogenous agents
24 without requiring needles³², gases³³, or other mechanisms¹⁰.

1

2 Delivery of therapeutics to the cells in the tissue will require UmTDD to facilitate transit through
3 the mucus layer³⁴. This could be achieved with mucus-penetrating particles (MPPs), which mimic
4 essential surface properties of viruses that prevent muco-adhesion^{30,35}. Combining drugs with MPPs
5 could facilitate their passage through the mucus layer, and insonation could further enhance drug
6 uptake into cells and/or through intercellular junctions. Similarly, the inclusion of mucolytic agents
7 in the capsule is another alternative approach to facilitate the delivery of drugs into cells and tissue.
8 Furthermore, the delivery of therapeutic agents in pathological areas such as inflamed tissue may
9 be sufficient with this method due to the diminished mucus layer in these regions³⁶.

10

11 Our results demonstrated that specific positions in the GI tract could be marked using focused US.
12 Marking tissue to help target subsequent interventions to a specific site is a potentially useful
13 approach to deliver treatment to a diseased site with a second follow-up capsule or surgically³⁷. A
14 capsule-based system could potentially locate diseased regions with microultrasound imaging³⁸, and
15 mark them with fluorescent particles in a US-mediated process. The fluorescently-marked
16 (diseased) regions could then be readily identified during surgery or with a second capsule capable
17 of fluorescence imaging^{39,40}. Such a secondary capsule could also deliver therapeutic agents to the
18 diseased site.

19

20 **Methods**

21 **Ultrasound Transducer Design and Fabrication**

22 A previously described prototype tethered capsule (Figure 1e) contained a focused US transducer,
23 white light imaging camera, LED-based illumination, and a drug delivery channel²²⁻²⁴. This capsule

1 was unsuitable for use *in vivo* as the tether was too short and inflexible, and the capsule could not
2 be made biocompatible. Additionally, because of the diameter of the capsule relative to that of the
3 porcine small bowel, the capsule will inevitably be in contact with the mucosa, which required it to
4 be redesigned to allow the US focus to be at the mucosa and not below it, deeper in the tissue. This
5 was achieved by recessing the transducer into the capsule, positioning the focus 1 mm from the
6 capsule perimeter, instead of 4 mm as in previous designs. The additional space required for the
7 recess meant that the new capsule (Figure 1d), could contain only a focused US transducer and drug
8 delivery channel, and no camera or illumination. Importantly, the dimensions of the capsule (11 mm
9 diameter, 3 mm length), remained comparable to those that are used clinically for visual diagnosis
10 such as the PillCam® SB (Medtronic Inc., Minneapolis, MN, USA) and PillCam® Colon
11 (Medtronic Inc., Minneapolis, MN, USA).

12

13 The transducer was produced using a curved PZ26 piezoceramic bowl (Meggitt A/S, Kvistgaard,
14 Denmark) intended for US transmission. Each bowl had a stated transmission frequency, $f = 4$ MHz,
15 an outer diameter of 5 mm, a radius of curvature of 15 mm, and an inner hole diameter of 1 mm.
16 The hole accommodates the delivery channel used for introducing therapeutic agents. The bowl was
17 contained in a case providing structural support that was created from VeroWhite material using the
18 Object Connex (Stratasys Ltd., Eden Prairie, MN, USA) additive manufacturing system. The case
19 was constrained to fit within the shell of an ingestible capsule, with shell dimensions no more than
20 11 mm in diameter and 30 mm in length. The case was designed in two parts to facilitate assembly
21 and insertion of the transducer. The first part was the main body that provided support for the
22 piezoceramic bowl and a supportive backing layer, with an outer diameter of 8 mm, and a length of
23 3 mm. The second part was a cap attached to the rear of the main body with an outer diameter of 8

1 mm, a thickness of 1 mm, and an inner hole diameter of 2 mm to allow the power cable and delivery tube for exogenous agents to pass through.

3
4 The silver electrode on the rear of the PZ26 bowl, as supplied by the manufacturer, was connected
5 to the inner conductor of a coaxial cable (813-3426, RS Components, Corby, UK) with outer
6 diameter of 1.17 mm, and length of 3.5 m, using conductive Ag-filled epoxy (G3349, Agar
7 Scientific, Stansted, UK). The distal end of the coaxial cable inner connector was attached to the
8 central pin of a cable-mount SMA connector (468-3075, RS Components, Corby, UK) using
9 conductive Ag-filled epoxy which was subsequently cured in an oven at 80°C for 15 minutes. The
10 backing layer was a very low acoustic impedance mixture of glass microbubbles (K1, 3M,
11 Maplewood, MN, USA) and epoxy (EpoFix, Struers A/S, Ballerup, Denmark) at a mass ratio of 1:3
12 intended to provide physical support with minimal ultrasonic damping. The backing layer was
13 applied to the rear surface of the PZ26 bowl inside the transducer case, and this was transferred to
14 an oven to cure for 15 minutes at 70°C. Once cured, a hole of approximate diameter 1 mm was
15 drilled through the backing layer using a 1 mm diameter drill bit to allow the delivery channel to
16 pass through it. Polythene tubing (Smith Medical Ltd., Cumbernauld, Scotland, UK) with an outer
17 diameter of 0.96 mm, an inner diameter of 0.58 mm, and a length of 3.5 m was used as the delivery
18 channel. The delivery channel tubing was passed through the backing layer and PZ26 bowl until it
19 was level with the front surface of the bowl and then fixed in place using EpoFix epoxy.

20
21 The second part of the transducer casing was attached to the rear of the main case using EpoFix
22 epoxy. The coaxial cable and delivery channel were passed through the central hole in the case. The
23 electrical ground connection was supplied by the outer connector of the coaxial cable attached to
24 the front surface electrode of the PZ26 bowl using conductive Ag-filled epoxy. This connector was

1 passed through a groove in the external surface of the case. The distal end of the outer coaxial cable
2 was attached to the outside of the cable mount SMA connector using conductive Ag-filled epoxy
3 and cured in an oven for 15 minutes at 80°C.

4

5 **Ultrasound field mapping**

6 The spatial distribution of the US field produced by the focused US transducers was mapped using
7 a commercial US field mapping (USFM) measurement system (Precision Acoustics Ltd.,
8 Dorchester, UK). The USFM system, as shown in Supplementary Figure 1, consisted of a needle
9 hydrophone (Precision Acoustics Ltd., Dorchester, UK) moved throughout the acoustic field,
10 including the focal region, to quantify the acoustic pressure distribution. The USFM system allows
11 motion along x , y , and z axes with a resolution of 3.8 μm . The system was controlled, and data
12 captured by a dedicated computer program produced with LabVIEW (National Instruments, Austin,
13 TX, USA). A focused US transducer was placed facing downwards in the USFM water tank
14 containing degassed water. The needle hydrophone that was used (Precision Acoustics Ltd.,
15 Dorchester, UK) had a sensitive area of diameter $\varnothing = 0.2$ mm and was positioned perpendicular to
16 the transducers' active element, and the motion step size was set to be 0.1mm, approximately 1/3 of
17 the wavelength. During USFM measurement, the focused US transducers were driven at the central
18 frequency by a 33210A signal generator (Keysight Technologies, Santa Rosa, CA, USA), and the
19 input was a continuous sine wave, varied from 1 – 10 V_{pp} , in 1 V_{pp} increments. A continuous sine
20 wave was used to promote cavitation effects. The peak-to-peak output voltage (V_{pp}) was recorded
21 from the hydrophone and analyzed offline for pressure conversion using code produced with
22 MATLAB (The MathWorks Inc., Natick, MA, USA). The USFM code also produced surface plots

1 of the pressure distribution and calculated the beam diameter at -6 dB. The uncertainty in
2 measurement at the appropriate frequency range is ± 1.5 dB.

3

4 **Acoustic power measurement of transducers**

5 Output acoustic power from the focused US transducers was measured using a commercial radiation
6 force balance (RFB) (Precision Acoustics Ltd., Dorchester, UK) set up with a conical acoustic
7 absorbing target. The power range of the system was 10 mW–100 W, and the frequency range was
8 1–10 MHz. The absorbing target was suspended in a tank of degassed water, and the transducer was
9 mounted on a stand facing downwards toward the absorbing target. The transducer was lowered
10 until the distance between the transducer and acoustic absorber was equal to the geometric focal
11 distance of the transducer. The transducer was powered by a 33210A signal generator (Keysight
12 Technologies, Santa Rosa, CA, USA). Due to the high sensitivity of the RFB system, it was encased
13 in a draught shield to prevent airflow disturbances and minimize variation. The RFB was connected
14 to a dedicated computer running LabVIEW software (National Instruments, Austin, TX, USA) for
15 data acquisition and analysis. The program directly provides acoustic output power W_{OUT} ,
16 considering factors such as frequency, transducer geometry, and water temperature when analyzing
17 the data. The uncertainty in measurement at the appropriate frequency range is $\pm 7\%$. The linearity,
18 efficiency, and intensity were calculated using W_{OUT} . The linearity was obtained by comparing
19 W_{OUT} measured by the RFB with the electrical input power, W_{IN} , driving the transducer. W_{IN} was
20 calculated using Equation 1.

21

$$W_{IN} = \frac{V_{RMS}^2}{z} = \frac{\left(\frac{V_{PP}}{2\sqrt{2}}\right)^2}{z} \quad \text{Equation 1}$$

1 where V_{RMS} is the root mean square input voltage, and Z is the electrical impedance magnitude at
2 the relevant frequency. The efficiency was calculated using Equation 2, where W_{OUT} is the average
3 US output power,

$$4 \quad \text{Efficiency} = \frac{W_{OUT}}{W_{IN}} \quad \text{Equation 2}$$

5 The acoustic intensity was then calculated using Equation 3:

$$6 \quad I = W_{OUT} / A \quad \text{Equation 3}$$

7 where A is the beam area at the transducer focal plane, taken at -6 dB.

8 **Testing of Ultrasound-mediated Delivery Transducers in *Ex Vivo* Tissue**

9 14 CL57BL/6 wild type and 14 $Apc^{Min/+}$ mice, with ages in the range of 50 - 110 days for WT (mean
10 85) and 55 and 95 days (mean 70) for $Apc^{Min/+}$, with 12/14 and 10/14 female for WT and $Apc^{Min/+}$,
11 respectively, were sacrificed by cervical dislocation. All experiments involving mice were
12 performed in accordance with UK Home Office approved guidelines and were approved by the
13 Home Office Licensing committee (Project license P3800598E), which operates in accordance with
14 the Animals (Scientific Procedures) Act 1986 (ASPA). The entire intestine was excised via
15 abdominal laparotomy and immediately placed in PBS at 4°C to maintain tissue quality. The lumen
16 was flushed with cold PBS with a syringe (Becton, Dickson and Company, Franklin Lakes, NJ,
17 USA). The small intestine was divided into sections measuring 80–100 mm and cut along the long
18 axis to expose the mucosa. Each sample was pinned to the acoustic absorber (shown in
19 Supplementary Figure 2) using 25-gauge hypodermic needles (Becton, Dickson and Company,
20 Franklin Lakes, NJ, USA), with the mucosa facing upwards. The correct orientation of the tissue
21 was confirmed through inspection with a dissection microscope. The tissue pinned to the acoustic
22 absorber was placed into the insonation tank (Supplementary Figure 2) and submerged in 250 ml
23 PBS at 37°C. The tank was then transferred to the insonation system

1
2 Quantum dots (product no. 753866, Sigma-Aldrich Corporation, St. Louis, MO, USA) with a
3 diameter of 6 nm, and an emission wavelength, $\lambda_{EM} = 540$ nm, were prepared in solution with PBS
4 at a concentration of 100 $\mu\text{g/ml}$. The QD solution was transferred to a 5 mL syringe (Becton,
5 Dickson and Company, Franklin Lakes, NJ, USA) and placed in the insonation system syringe
6 driver. This QD only solution was introduced through the transducer delivery channel at a rate of 1
7 mL/min for 60 s. A 10 V_{pp} continuous sinusoidal waveform was applied to the transducer for 60 s
8 per sample, producing the specific acoustic parameters presented in Table 1. Control samples
9 consisted of a QD solution transferred onto tissue under the same conditions as above but without
10 insonation. Additionally, the order of insonated and control samples was alternated in different
11 experiments to account for any changes introduced by possible tissue degradation during
12 experiments. Immediately after sonication, tissue was clamped and prepared for fixation
13
14 Additional *ex vivo* experiments were also conducted on sections of the small intestine obtained from
15 WT pigs, where the acoustic parameters shown in Table 2 were measured to be generated by the
16 same 10 V_{pp} continuous sinusoidal waveform. Sixteen small intestine sections were obtained from
17 9 pigs, aged 4 – 6 months and weighing 40 – 60 kg. Before death, the animals were used in GI
18 experiments and killed using pentobarbital. *Post mortem* samples were obtained and used within
19 20 minutes to minimize tissue degradation. The small intestine section was excised via abdominal
20 laparotomy and placed in PBS at 4°C immediately. The section was cut along the long axis to expose
21 the mucosa and washed three times with PBS at 37°C. It was then cut into smaller sections, 50–75
22 mm in length and pinned to the acoustic absorber using 25-gauge hypodermic needles (Becton,
23 Dickson and Company, Franklin Lakes, NJ, USA), mucosa facing up. The remaining length of the
24 small intestine was stored at 4°C in PBS until insonation. The pinned tissue section was placed in

1 the insonation tank, and a solution of 250 ml PBS at 37°C was added. The remainder of the
2 experiment followed the protocol described for the murine samples.

3
4 Immediately post insonation/QD exposure, samples were washed with 37°C PBS using gentle
5 agitation and rinsed using a syringe containing 37°C PBS, whilst taking care not to damage the
6 mucosa. Samples were viewed under a 350 nm ultraviolet (UV) lamp (UVGL-58, UVP LLC,
7 Upland, CA, USA) to assess QD uptake, and images were recorded with a digital camera. Post
8 imaging, the method used to fix the tissue samples varied.

9
10 For immunofluorescence staining to determine the location of the QDs in murine tissue, the protocol
11 detailed above for murine tissue was repeated but with a MB/QD solution that consisted of 5% QDs
12 and 5% MBs in PBS. This MD/QD solution was introduced through the transducer delivery channel
13 at a rate of 1 mL/min for 60 s. A 10 V_{pp} continuous sinusoidal waveform was applied to the
14 transducer for 90 s per sample. Control samples were also produced whereby the MB/QD solution
15 was provided through the transducer delivery channel at the same rate but without the presence of
16 ultrasound. The order of control and insonated samples was varied to account for the effects of tissue
17 degradation during the experiment. After the experiment, the small intestine samples were placed
18 into either 4% PFA in PBS (Sigma-Aldrich Corporation, St. Louis, MO, USA) or Carnoy's fixative,
19 which is better able to preserve the mucus layer by fixing the mucin, and were cryoprotected
20 overnight in a solution of 30% sucrose in PBS. The tissue was cut into 1mm pieces and placed in
21 cryomolds before being left to incubate in 361603E OCT (VWR International, Radnor, PA, USA)
22 for 30 minutes. The tissue was placed in the cryostat at -20°C and left to freeze before being
23 mounted on microtome chucks using OCT. The small intestine was cut into 10-12 µm sections, with
24 2 to 3 sections placed onto Leica X-tra adhesive microscope slides (Leica Biosystems Nussloch

1 GmbH, Nußloch, Germany) and left to air dry for 10 minutes and stored at -20°C . The edges of the
2 section were blocked with a PAP pen and washed in PBS. The sections were incubated in Texas
3 Red conjugated WGA (10 $\mu\text{g}/\text{ml}$) with Hoechst (1 $\mu\text{g}/\text{ml}$) for 60 minutes before being mounted
4 using Vectashield anti-fade non-setting mounting agent and imaged using a Zeiss LSM 710 or LSM
5 880 laser scanning confocal microscopy (Carl Zeiss AG, Oberkochen, Germany). All sections were
6 examined for QDs in the tissue. For the small intestine, two areas were sectioned and examined
7 along the entire length of the section (area Q1 = 5,400 μm , Q2 = 22,500 μm).

8

9 **Design and Fabrication of Ultrasound-mediated Delivery Capsule**

10 The capsule shell was designed in two parts, with pins locking the two halves together (Figure 1b).
11 The capsule had a port to attach the tether and provide extra attachment strength. The transducer
12 slot was at an angle such that the focus of the transducer was 1 mm radially distant from the capsule
13 perimeter. This means that the transducer was focused on the luminal surface of the gut wall when
14 the capsule was in contact with the wall of the GI tract³⁸. The capsule was constructed in VeroWhite
15 material using an Objet Connex 500 printer (Stratasys Ltd., Eden Prairie, MN, USA).

16

17 A tether was necessary to house the transducer power cable and the delivery channel. The tether had
18 to be flexible enough to prevent distention of the small intestinal wall, which could potentially affect
19 results but also be stiff enough to allow it to be used to push the capsule²³ into the small intestine.
20 One lesson learned from the earlier capsule is that the tether, a repurposed vascular catheter, was
21 too stiff to be used in the GI tract *in vivo*. Instead, the tether for the present capsule was a nasoenteric
22 feeding tube (Corpak Medsystems Inc., Alpharetta, GA, USA) with an outer diameter of 3.3 mm,
23 an inner diameter of 2.5 mm, and length of 1.4 m. This tube was flexible but stiff enough to allow

1 the capsule to be pushed into and along the small intestine. The tubing had a graduated scale printed
2 on the outside and was marked every 1cm, making it possible to determine approximately how far
3 the capsule had been inserted. This tubing allowed the capsule to be inserted up to 1.4 m into the
4 porcine GI tract, thus leaving a further 2.0 m of an external transducer power cable and delivery
5 channel connecting to control equipment. The extra cable ensured adequate space between the pig
6 and measurement equipment during the *in vivo* experiments.

7

8 Medical grade epoxy (EP42HT-2MED, Master Bond Inc., Hackensack, NJ, USA) was manually
9 dispensed by a syringe into the transducer and tether slot in one half of the capsule shell. The
10 transducer and tether were secured in the slot (Figure 1b), and the epoxy was left to cure overnight
11 at room temperature. The same medical-grade epoxy was also used to join both parts of the capsule
12 shell together and left to cure overnight at room temperature. The fully assembled capsules (Figure
13 1c) were visually inspected for voids, and then medical grade epoxy was applied to the interfaces
14 and left to cure at room temperature overnight.

15

16 As VeroWhite is not biocompatible, an 8 μm thick conformal coating of Parylene C was applied to
17 the assembled capsule to not only ensure biocompatibility but also to reduce friction between the
18 capsule and the wall of the GI tract. Parylene C was deposited using a vacuum deposition tool (SCS
19 PDS 2010, Specialty Coating Systems, IN, USA). The surfaces were primed with A174 silane
20 adhesion promoter before deposition. Parylene C is a USP Class VI polymer that is commonly used
21 for coating medical devices such as surgical instruments, implants, and medical electronics⁴¹.

22

1 ***In vivo* Testing of Ultrasound-mediated Delivery Capsule**

2 The performance of the capsule was measured using *in vivo* porcine models. The experiments were
3 conducted in collaboration with the Wellcome Trust Critical Care Laboratory for Large Animals
4 (Roslin Institute, Roslin, Scotland, UK) under license from the UK Home Office (PPL 70/8812).
5 The experiments were approved by the Animal Welfare and Ethical Review Board of the Roslin
6 Institute and were carried out in compliance with the terms of the Home Office license and the
7 Animals (Scientific Procedures) Act 1986 (ASPA). Four female pigs were used with ages in the
8 range of 3 to 6 months and weighed between 40 kg and 55 kg (Table 3).

9
10 Anesthesia was induced with isoflurane (Zoetis Inc., Parsippany-Troy Hills, NJ, USA), vaporized
11 in nitrous oxide and oxygen, and administered using a Bain breathing system. A cannula was
12 inserted into the auricular vein and the trachea was intubated. Anesthesia was maintained with
13 isoflurane. Ringer's lactate solution (Aquapharm No. 11, Animalcare UK Ltd., North Yorkshire,
14 UK) was administered throughout the study at 10 ml/kg/h. Normocapnia was maintained with
15 mechanical ventilation of the porcine lungs. Vital signs were continuously monitored through the
16 duration of the experiment by an experienced veterinary anesthetist. A stoma was created using the
17 in-house protocol to allow direct access to the small intestine from the abdomen, bypassing the
18 esophagus and stomach. The small intestine was flushed with PBS through the stoma. Lubrication
19 to facilitate capsule insertion was provided by a saline drip (0.9% by weight, 1-2 drops/s) at the
20 stoma entrance.

21
22 The transducer power cable was connected to a DG4102 signal generator (RIGOL Technologies,
23 Beijing, China) and the capsule delivery channel was connected to a NE-1000 syringe driver (New
24 Era Pump Systems Inc., New York City, NY, USA) containing a syringe with MB/QD solution

1 comprising 50 µg/ml QDs (753866, Sigma Aldrich Corporation, St. Louis, MO, USA) and 1×10^6
2 MBs/mL (SonoVue MBs (Bracco Imaging, Milan, Italy) MB Ø 2 - 9 microns) in the provided
3 physiological saline, as shown in the system diagram in Figure 5.

4

5 Each capsule was inserted through the stoma to a maximum distance at which it was difficult to
6 manipulate the tether through the looping intestine. The distances achieved ranged from 40–75 cm
7 (Table 3). The capsule was then removed from the stoma and cleaned with PBS. This step was
8 necessary to assess the level of bowel preparation. A poorly cleaned bowel impeded capsule
9 advancement and adversely affected insonation results. The capsule was primed before re-insertion
10 by running a 2 ml MB/QD solution through the delivery channel to ensure it was not obstructed.
11 The capsule was re-inserted into the small intestine to the maximum distance achievable and pulled
12 back towards the stoma in positional increments of 10 cm, measured using the scale on the tether,
13 with ‘treatment’ was delivered at each position. Different insonation/control parameters were
14 applied at each incremental position to deliver the QDs, with the final location 10 cm from the stoma

15 (

1 Table 4). To test each set of parameters required 30 cm of small intestine. Therefore, the maximum
2 number of experimental sets achievable per pig was two due to the maximum penetration depth
3 achieved. Once all experiments were completed, the animals were euthanized while anesthetized
4 using pentobarbital (Akorn Pharmaceuticals, Lake Forest, IL, USA).

5

6 **Mucosal analysis**

7 Once death was confirmed, small intestine sections were removed via abdominal laparotomy. The
8 sections that had been sonicated were identified by measuring the distance from the stoma. Sections
9 were cut along the long axis and placed on a tray, mucosa facing upward. These sections were placed
10 in PBS at 4°C immediately. The tissue was washed three times with PBS at 37°C, taking care not
11 to damage the mucosa. The tissue was taken to a dark room and visualized under 350 nm UV light
12 using a UV lamp (UVGL-58, UVP LLC, Upland, CA, USA). Images were acquired using a digital
13 camera. Post-imaging, tissue samples were fixed in freshly prepared 4% PFA, pre-warmed to 37°C,
14 for 10 minutes. After fixing, tissue was permeabilized with 1 ml permeabilization buffer (2% TX100
15 in PBS) in a 2 ml Eppendorf tube for 2 hours on a rocking table before washing (3 x 20 min) in PBS.
16 1ml of staining solution consisting of phalloidin and DAPI (Table 5) was added. PBS was added to
17 each sample in a 2 ml Eppendorf tube wrapped in foil and left for 72 hours on a rocking table at
18 4°C. After staining, samples were washed 3 x 20 min in PBS on a rocking table. Samples were
19 imaged using a Zeiss 710 confocal microscope (Carl Zeiss AG, Oberkochen, Germany) and Z-stacks
20 were taken at the appropriate locations for each sample.

21

22 **References**

- 23 1. Borner, M. . *et al.* Patient preference and pharmacokinetics of oral modulated UFT versus
24 intravenous fluorouracil and leucovorin. *Eur. J. Cancer* **38**, 349–358 (2002).
- 25 2. Wilson, C. G. & Crowley, P. J. *Controlled Release in Oral Drug Delivery*. (Springer US,
26 2011). doi:10.1007/978-1-4614-1004-1.
27

- 1 3. Vllasaliu, D., Thanou, M., Stolnik, S. & Fowler, R. Recent advances in oral delivery of
2 biologics: nanomedicine and physical modes of delivery. *Expert Opin. Drug Deliv.* **15**,
3 759–770 (2018).
- 4 4. Moroz, E., Matoori, S. & Leroux, J.-C. Oral delivery of macromolecular drugs: Where we
5 are after almost 100 years of attempts. *Adv. Drug Deliv. Rev.* **101**, 108–121 (2016).
- 6 5. Goldberg, M. & Gomez-Orellana, I. Challenges for the oral delivery of macromolecules.
7 *Nat. Rev. Drug Discov.* **2**, 289–295 (2003).
- 8 6. Podolsky, D. K. Inflammatory Bowel Disease. *N. Engl. J. Med.* **325**, 928–937 (1991).
- 9 7. Kaur, G., Arora, M. & Ravi Kumar, M. N. V. Oral drug delivery technologies—a decade of
10 developments. *J. Pharmacol. Exp. Ther.* **370**, 529–543 (2019).
- 11 8. Traverso, G. *et al.* Microneedles for drug delivery via the gastrointestinal tract. *J. Pharm.*
12 *Sci.* **104**, 362–367 (2015).
- 13 9. Cummins, G. *et al.* Gastrointestinal diagnosis using non-white light imaging capsule
14 endoscopy. *Nat. Rev. Gastroenterol. Hepatol.* **16**, 429–447 (2019).
- 15 10. Steiger, C. *et al.* Ingestible electronics for diagnostics and therapy. *Nat. Rev. Mater.* **4**, 83–
16 98 (2019).
- 17 11. van der Schaar, P. J. *et al.* A novel ingestible electronic drug delivery and monitoring
18 device. *Gastrointest. Endosc.* **78**, 520–528 (2013).
- 19 12. Parr, A. F. *et al.* Evaluation of the feasibility and use of a prototype remote drug delivery
20 capsule (RDDC) for non-invasive regional drug absorption studies in the GI tract of man
21 and beagle dog. *Pharm. Res.* **16**, 266–71 (1999).
- 22 13. Wilding, I. *et al.* Development of a new engineering-based capsule for human drug
23 absorption studies. *Pharm. Sci. Technol. Today* **3**, 385–392 (2000).
- 24 14. Lentacker, I., De Cock, I., Deckers, R., De Smedt, S. C. & Moonen, C. T. W.
25 Understanding ultrasound induced sonoporation: Definitions and underlying mechanisms.
26 *Adv. Drug Deliv. Rev.* **72**, 49–64 (2014).
- 27 15. Hernot, S. & Klibanov, A. L. Microbubbles in ultrasound-triggered drug and gene delivery.
28 *Adv. Drug Deliv. Rev.* **60**, 1153–1166 (2008).
- 29 16. Dimcevski, G. *et al.* A human clinical trial using ultrasound and microbubbles to enhance
30 gemcitabine treatment of inoperable pancreatic cancer. *J. Control. Release* **243**, 172–181
31 (2016).
- 32 17. Escoffier, J.-M. & Bouakaz, A. *Therapeutic Ultrasound*. (Springer International Publishing,
33 2016). doi:10.1007/978-3-319-22536-4.
- 34 18. Ho, L., Bokharaei, M. & Li, S.-D. Current update of a thermosensitive liposomes composed
35 of DPPC and Brij78. *J. Drug Target.* **26**, 407–419 (2018).
- 36 19. Chen, H. & Hwang, J. Ultrasound-targeted microbubble destruction for chemotherapeutic
37 drug delivery to solid tumors. *J. Ther. Ultrasound* **1**, 10 (2013).
- 38 20. Sirsi, S. R. & Borden, M. A. Microbubble compositions, properties and biomedical
39 applications. *Bubble Sci. Eng. Technol.* **1**, 3–17 (2009).
- 40 21. Schoellhammer, C. M. *et al.* Ultrasound-mediated gastrointestinal drug delivery. *Sci.*
41 *Transl. Med.* **7**, 310ra168-310ra168 (2015).
- 42 22. Stewart, F. *et al.* Development of a therapeutic capsule endoscope for treatment in the
43 gastrointestinal Tract: Bench testing to translational trial. in *2017 IEEE International*
44 *Ultrasonics Symposium (IUS)* 1–1 (IEEE, 2017). doi:10.1109/ULTSYM.2017.8092467.
- 45 23. Stewart, F. *et al.* A Prototype Therapeutic Capsule Endoscope for Ultrasound-Mediated
46 Targeted Drug Delivery. *J. Med. Robot. Res.* **03**, 1840001 (2018).
- 47 24. Stewart, F. R. *et al.* Acoustic sensing and ultrasonic drug delivery in multimodal theranostic
48 capsule endoscopy. *Sensors* **17**, 1553 (2017).
- 49 25. Barroso, M. M. Quantum dots in cell biology. *Journal of Histochemistry and Cytochemistry*
50 (2011) doi:10.1369/0022155411398487.
- 51 26. Rosenberg, D. W., Giardina, C. & Tanaka, T. Mouse models for the study of colon
52 carcinogenesis. *Carcinogenesis* (2009) doi:10.1093/carcin/bgn267.
- 53 27. Grivennikov, S. I. *et al.* Adenoma-linked barrier defects and microbial products drive IL-

- 1 23/IL-17-mediated tumour growth. *Nature* **491**, 254–258 (2012).
- 2 28. Fatehullah, A. *et al.* Increased variability in ApcMin/+ intestinal tissue can be measured
3 with microultrasound. *Sci. Rep.* **6**, 29570 (2016).
- 4 29. Turcanu, M. V. *et al.* Ultrasound and Microbubbles Promote the Retention of Fluorescent
5 Compounds in the Small Intestine. in *2018 IEEE International Ultrasonics Symposium*
6 *(IUS)* 1–4 (IEEE, 2018). doi:10.1109/ULTSYM.2018.8580036.
- 7 30. Lai, S. K., Wang, Y.-Y. & Hanes, J. Mucus-penetrating nanoparticles for drug and gene
8 delivery to mucosal tissues. *Adv. Drug Deliv. Rev.* **61**, 158–171 (2009).
- 9 31. Stride, E. P. & Coussios, C. C. Cavitation and contrast: The use of bubbles in ultrasound
10 imaging and therapy. *Proc. Inst. Mech. Eng. Part H J. Eng. Med.* (2010)
11 doi:10.1243/09544119JEIM622.
- 12 32. Abramson, A. *et al.* An ingestible self-orienting system for oral delivery of
13 macromolecules. *Science (80-.)*. **363**, 611–615 (2019).
- 14 33. Groening, R. & Bensmann, H. High frequency controlled capsules with integrated gas
15 producing cells. *Eur. J. Pharm. Biopharm.* **72**, 282–284 (2009).
- 16 34. Boegh, M. & Nielsen, H. M. Mucus as a Barrier to Drug Delivery - Understanding and
17 Mimicking the Barrier Properties. *Basic Clin. Pharmacol. Toxicol.* **116**, 179–186 (2015).
- 18 35. Ensign, L. M., Cone, R. & Hanes, J. Oral drug delivery with polymeric nanoparticles: The
19 gastrointestinal mucus barriers. *Adv. Drug Deliv. Rev.* **64**, 557–570 (2012).
- 20 36. Michielan, A. & D’Inca, R. Intestinal Permeability in Inflammatory Bowel Disease:
21 Pathogenesis, Clinical Evaluation, and Therapy of Leaky Gut. *Mediators of Inflammation*
22 (2015) doi:10.1155/2015/628157.
- 23 37. Cox, B. F., Stewart, F., Huang, Z., Nathke, I. S. & Cochran, S. Ultrasound facilitated
24 marking of gastrointestinal tissue with fluorescent material. in *2016 IEEE International*
25 *Ultrasonics Symposium (IUS)* 1–4 (IEEE, 2016). doi:10.1109/ULTSYM.2016.7728782.
- 26 38. Lay, H. *et al.* In-Vivo Evaluation of Microultrasound and Thermometric Capsule
27 Endoscopes. *IEEE Trans. Biomed. Eng.* **66**, 632–639 (2018).
- 28 39. Al-Rawhani, M. A., Beeley, J. & Cumming, D. R. S. Wireless fluorescence capsule for
29 endoscopy using single photon-based detection. *Sci. Rep.* **5**, 18591 (2015).
- 30 40. Beeley, J. *et al.* Imaging Fluorophore-Labelled Intestinal Tissue via Fluorescence
31 Endoscope Capsule. *Proceedings* **2**, 766 (2018).
- 32 41. Kuppusami, S. & Oskouei, R. H. Parylene Coatings in Medical Devices and Implants: A
33 Review. *Univers. J. Biomed. Eng.* (2015) doi:10.13189/ujbe.2015.030201.

34 **Acknowledgments**

35
36
37 Financial support is gratefully acknowledged from the UK Engineering and Physical Sciences
38 Research Council (EPSRC), Grant EP/K034537 (Sonopill Programme), and the Biotechnology and
39 Biological Sciences Research Council (BBSRC), Grant BB/M017079/1. Microscope access was
40 provided by the Dundee Imaging Facility; the Zeiss LSM 880 Airyscan microscope was funded by
41 an MRC grant to the Protein Phosphorylation and Ubiquitylation Unit.

42 **Author contributions statement**

43
44
45 F.S. conceived and conducted most experiments, designed and built the capsule, and analyzed
46 results. G.C. contributed to the design, manufacturing, and assembly of the capsule as well as
47 drafting the initial manuscript. M.T. conducted some of the experiments using mouse tissue; and
48 contributed to the design of experiments and analysis of results. B.C. prepared the mouse and tissue
49 for sonication, contributed to the design of experiments, conducted the *in-vivo* experiments, and
50 analyzed the results. A.P. processed, imaged, and analyzed the results of the cross-sectional imaging
51 of murine intestinal mucosa. I.P.N. conducted preliminary murine experiments, helped with data

1 acquisition from murine studies, and contributed to the design and running of those experiments.
2 E.C contributed to the design of the *in-vivo* experiments and conducted them. M.Y.P.D contributed
3 to the writing of the manuscript and provision of resources for the manufacturing and assembly of
4 capsules. M. Thanou contributed to the supervision and planning of all aspects of this work. HM
5 contributed to the planning and supervision of microbubble experiments and UmTDD delivery,
6 provision of equipment, and discussion of the results. SC contributed to the supervision and planning
7 of all aspects of this work, analysis of the experimental results, and provision of resources required
8 for the experiments. I.N. contributed to experiments, the writing of the manuscript, provision of
9 resources for biological experiments, and supervision of all aspects of this work. All authors
10 reviewed the manuscript.

11

12 **Additional information**

13

14 The authors declare no competing financial interests.

15

- 1 Table 1: Output parameters of the miniature focused ultrasound transducer used for the *ex-vivo*
2 tissue experiments

Voltage (V_{pp})	W_{IN} (mW)	W_{OUT} (mW)	Efficiency (%)	Acoustic Pressure (kPa)	IAC (Wcm⁻²)
3	20.1	9.6 ± 0.7	42.1 ± 3.3	344.5 ± 065.5	1.4 ± 0.0
4	35.8	20.2 ± 3.2	49.8 ± 3.9	443.4 ± 084.2	1.6 ± 0.1
5	55.9	31.3 ± 4.2	49.4 ± 3.9	544.7 ± 103.5	2.3 ± 0.1
6	80.5	42.4 ± 3.0	46.4 ± 3.7	636.3 ± 120.9	3.0 ± 0.2
7	109.6	56.8 ± 4.0	45.8 ± 3.6	741.3 ± 140.8	3.4 ± 0.2
8	143.1	76.6 ± 5.4	47.3 ± 3.7	826.8 ± 157.1	4.3 ± 0.3
9	181.1	92.5 ± 6.5	44.9 ± 3.6	917.4 ± 174.3	4.8 ± 0.4
10	223.6	115.1 ± 8.1	45.3 ± 3.6	1016.2 ± 193.1	6.1 ± 0.5

- 3
4 Table 2: Output parameters of the miniature focused ultrasound transducer used for the *in-vivo*
5 capsule.

Voltage (V_{pp})	W_{IN} (mW)	W_{OUT} (mW)	Efficiency (%)	Acoustic Pressure (kPa)	IAC (Wcm⁻²)
3	20.1	12.8 ± 1.0	42.1 ± 3.3	344.5 ± 065.5	1.0 ± 0.1
4	35.8	20.2 ± 3.2	49.8 ± 3.9	443.4 ± 084.2	1.4 ± 0.2
5	55.9	30.8 ± 4.2	49.4 ± 3.9	544.7 ± 103.5	2.2 ± 0.3
6	80.5	40.5 ± 4.0	46.4 ± 3.7	636.3 ± 120.9	2.9 ± 0.3
7	109.6	57.8 ± 4.3	45.8 ± 3.6	741.3 ± 140.8	4.2 ± 0.3
8	143.1	76.6 ± 5.6	47.3 ± 3.7	826.8 ± 157.1	5.4 ± 0.4
9	181.1	92.5 ± 6.6	44.9 ± 3.6	917.4 ± 174.3	6.5 ± 0.5
10	223.6	115.2 ± 8.1	45.3 ± 3.6	1016.2 ± 193.1	7.8 ± 0.6

- 6
7

- 1 Table 3: Detailed description of the four pigs used for *in vivo* delivery. Age, weight and the
- 2 maximum depth of insertion achieved by the capsule through the stoma are displayed

Pig Identification Number	Age (Months)	Weight (kg)	Maximum Depth of Insertion (cm)
20170921-P1	3-4	40.0	55.0
20170921-P2	3-4	40.0	40.0
20171109-P1	6	55.0	75.0
20171109-P2	6	52.0	55.0

3

1 Table 4: *In-vivo* experimental parameters

	Ultrasound Sine Wave Parameters			QD Flow Parameters	
	Frequency (MHz)	Amplitude (V _{pp})	Duration (s)	Flow Rate (mL/hr)	Duration (s, t ₀ = 30s)
Insonation	3.98	8.0	90 .0	60.0	60.0
Control	3.98	8.0	90 .0	NA	
Control	NA	NA	NA	60.0	60.0

2

1 Table 5: List of Immunofluorescent stains used

Material	Source	Cat. No.	Excitation	Emission	Label/Dye	Dilution or Concentration
Phalloidin	Invitrogen	A12380	578	600	Alexa Fluor 568	1:40
DAPI	Sigma-Aldrich	D9542	340	488	-	1:5000
WGA	Invitrogen	W21405	595	615	Texas Red-X	10 µg/ml

2

1 I. Figures

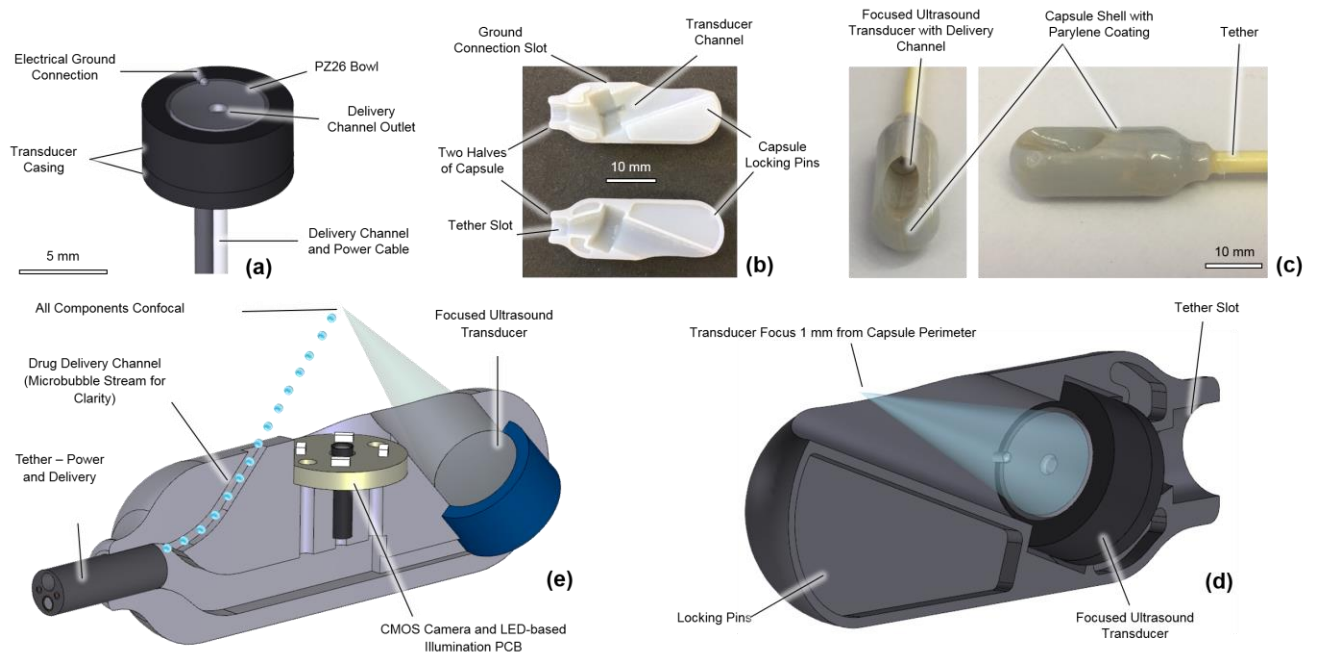


Figure 1: (a) Schematic of ultrasound transducer used in delivery capsule. (b) Locking mechanism for aligning capsule. (c) External view of capsule for *in vivo* drug delivery. (d) Cross-sectional image of *in vivo* delivery capsule. (e) Cross-sectional image of original prototype capsule²⁴.

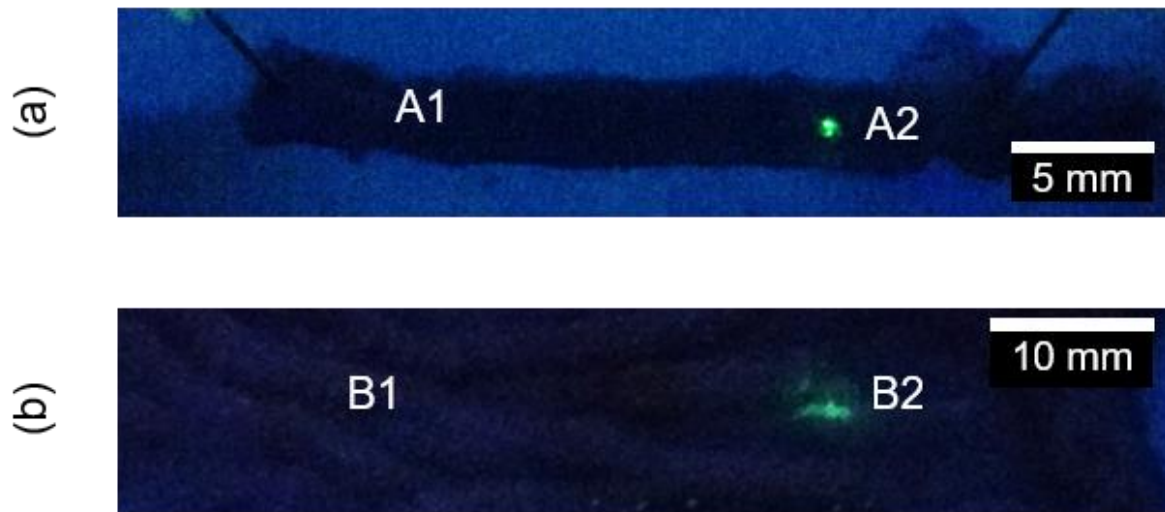


Figure 2: (a) Regions of wild type murine and (b) porcine intestine that were not-insonated (A1, B1) or insonated (A2, B2). In all cases tissue was exposed to Quantum dots. Quantum dots were clearly visible only when tissue was insonated (A2 and B2).

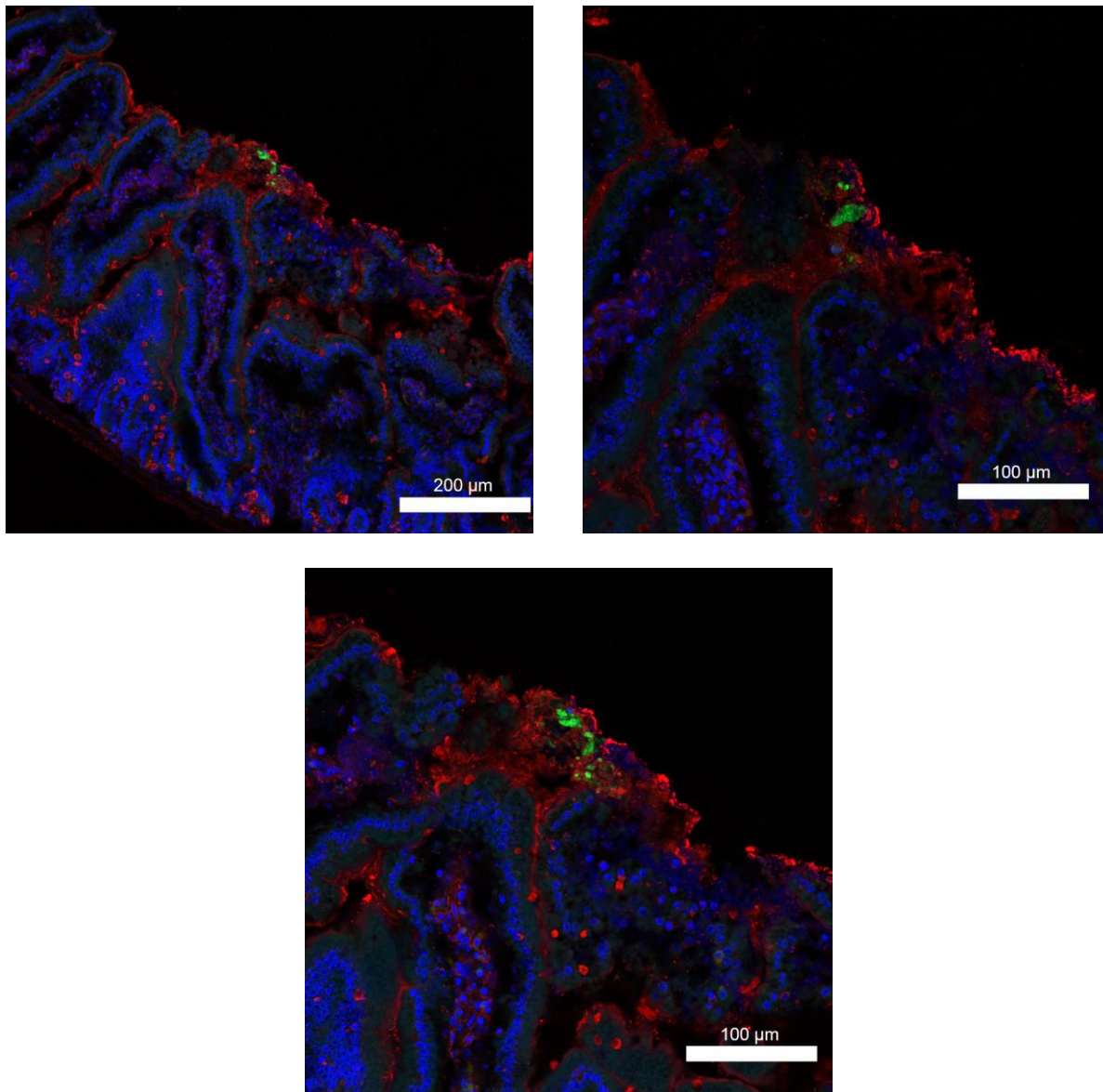
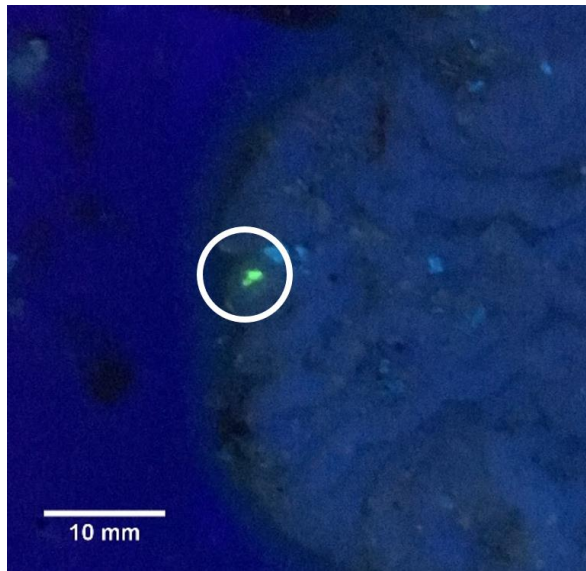
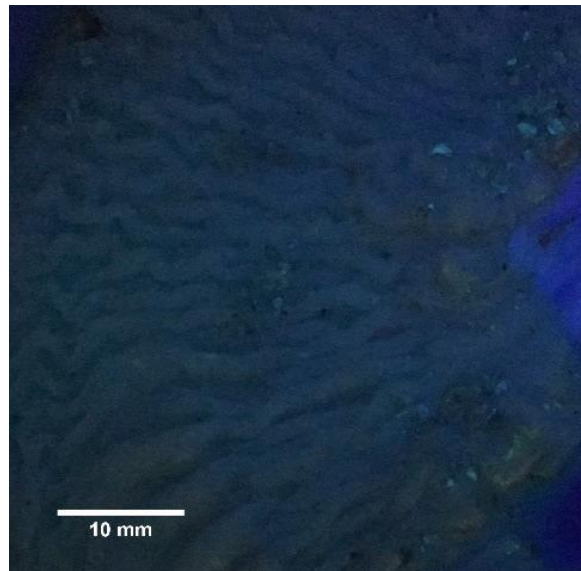


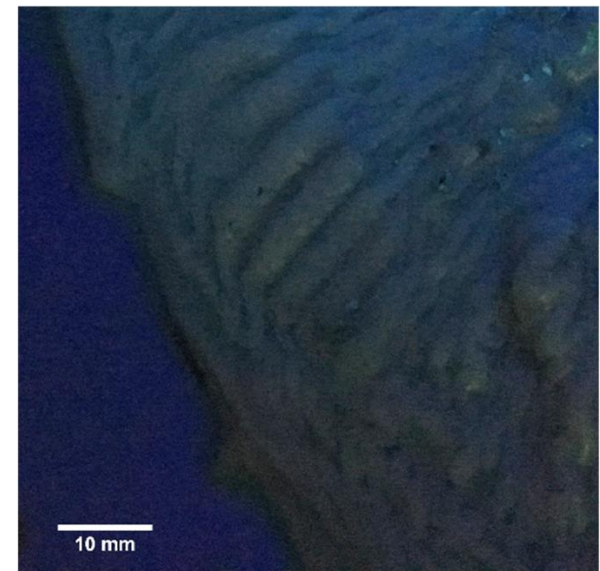
Figure 3: Cross-sections of different examples of murine small intestine after insonation with QDs and MBs. Images show QDs (green) are lodged in the mucosa (stained with WGA, red) after insonation and did not penetrate the underlying intestinal tissue (marked by DNA stain to show nuclei, blue).



(a)

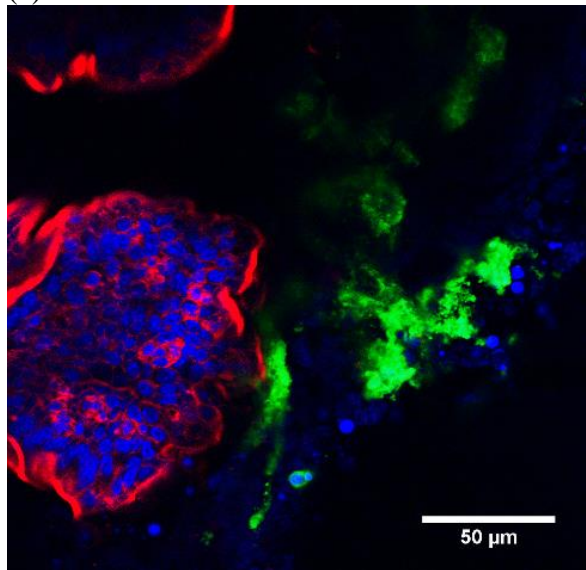


(b)

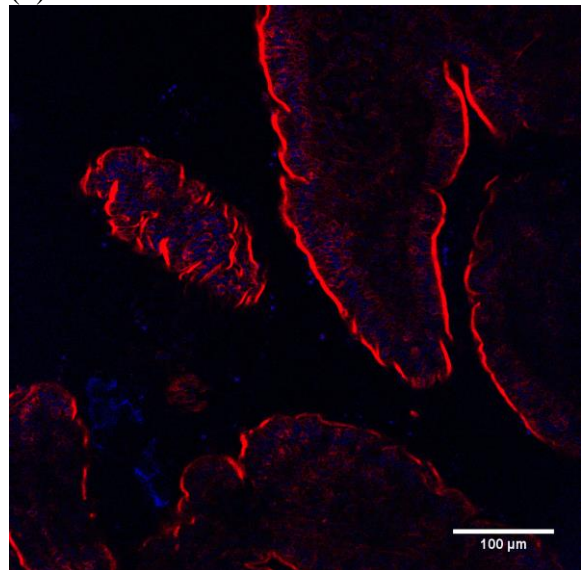


(c)

Quantum Dots (QDs): Green
 Actin (phalloidin): Red
 Nuclei (dapi): Blue



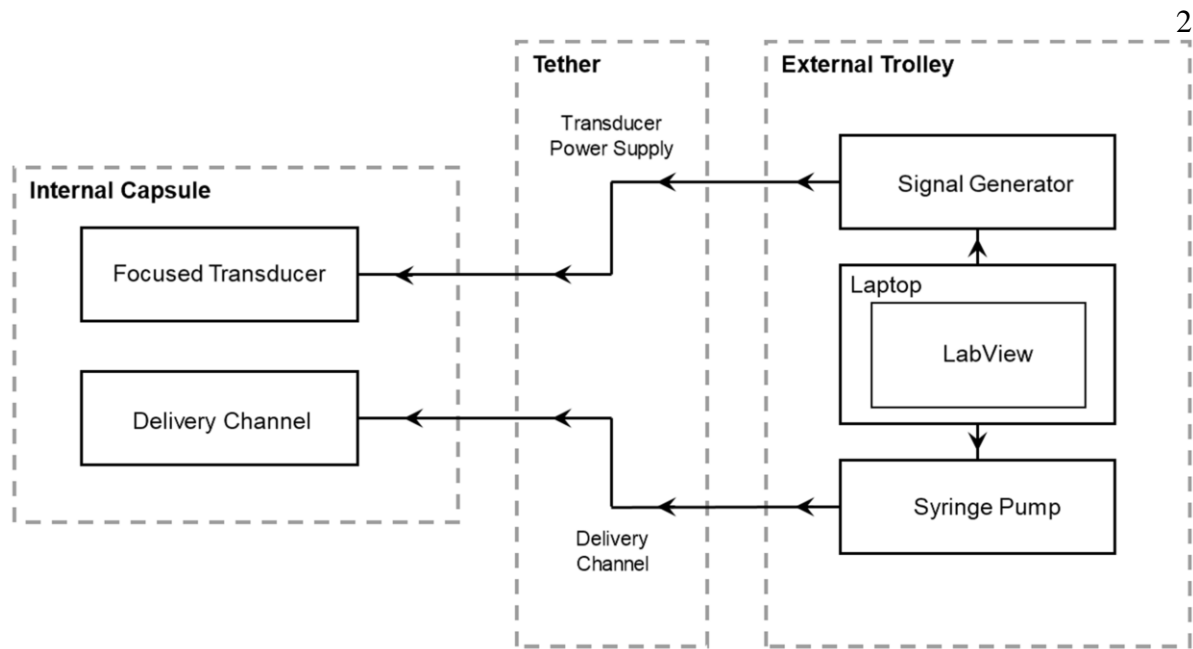
(d)



(e)

Figure 4: (a - c) Tissue from animal 20170921-P1. (a) Tissue sections exposed to insonation and QDs (white circle). (b) Tissue from area exposed to insonation only (no QDs). (c) Tissue from area exposed to QDs only. (d, e) Immunofluorescent staining of samples (a) and (c). The QDs were never detected inside epithelial cells marked by F-actin (red), which is highly concentrated in the apical brush border. Images a, b and c are reproduced with permission from ²⁹

1



2

Figure 5: Schematic diagram of the capsule setup for the *in vivo* trial.

20

21

22

23

24